MINDLIN PLATE THEORY: BEST SHEAR COEFFICIENT AND HIGHER SPECTRA VALIDITY

N. G. STEPHEN

Department of Mechanical Engineering, University of Southampton, Highfield, Southampton SO17 1BJ, England

Mindlin plate theory predicts three frequency spectra or, equivalently, three branches to a phase velocity dispersion diagram, the lowest of which—the w_1 mode—provides rotatory inertia and shear deformation corrections to classical thin plate theory. Employing consistent truncation procedures to both the Mindlin and the exact Rayleigh–Lamb frequency equations, valid for long wavelength and low phase velocity, one finds that w_1 mode agreement is achieved when the shear coefficient takes the value $\kappa = 5/(6 - v)$; the Mindlin prediction is then less than -0.5% in error when the wavelength is equal to the plate thickness, and less than $+1\%$ in error as wavelength approaches zero. The previously dismissed Mindlin H mode is seen to be in exact frequency (or phase velocity) agreement with the second slowest SH wave in the infinite plate, as long as the shear coefficient for this mode takes the value $\kappa = \pi^2/12$. However the w_2 mode, as with the second frequency spectrum of Timoshenko beams, should be regarded as the inevitable, but meaningless, consequence of an otherwise remarkable approximate engineering theory.

© 1997 Academic Press Limited

1. INTRODUCTION

The purpose of this paper is to address two issues concerning Mindlin Plate Theory (MPT) [1, 2], neither of which is new to the literature. These are (a) what is the "best" shear coefficient, and (b) what is the validity of the so-called w_2 and H modes, these being the second and third frequency spectra predicted by MPT. The approach adopted in the paper follows closely that taken by the present author in addressing the same two issues in relation to Timoshenko Beam Theory (TBT). Thus the "best" shear coefficient is here defined as that which will provide agreement of phase velocity (or, equivalently, natural frequency for a standing wave) with the appropriate exact (according to the spirit of the linear theory of elasticity) theory for the lowest flexural mode of vibration, when both theories are approximated by a consistent truncation procedure designed to include all second order effects*. (It should be noted, however, that this definition does not necessarily ensure "best" agreement between other aspects of the vibration; for example, maximum stress.) In the case of a Timoshenko beam this procedure, see reference [3], provided the shear coefficients

$$\kappa = 6(1 + v)^2/(7 + 12v + 4v^2) \qquad \text{and} \qquad \kappa = 5(1 + v)/(6 + 5v) \qquad \text{(1a, b)}$$

for the beam of circular and thin rectangular (plane stress) cross-sections, respectively; the exact theories employed were due to Pochhammer and Chree (see, for example, reference [4]), for the circular cross-section, and a plane stress version of the (plane strain)

---

* These truncation procedures were first employed by Timoshenko (see, for example, reference [22]), but the final step, that of matching the two second order approximations, was not taken.

Rayleigh–Lamb theory for the plate, due to Cowper [5]. Experimental support for these as the "best" coefficients, in terms of frequency, has been provided by Kaneko [6]. After having established the "best" coefficients for the two cases in which exact theories were available, a procedure was then required which would predict similar "best" coefficients for beams of cross-section other than circular and thin rectangular; this was done in reference [7], where a second order beam theory was produced in which the shear stress distribution during flexural vibration was approximated *not* by that of Saint-Venant flexure, that is a beam subjected to a constant shearing force, as had been done by Cowper [8], but rather it was assumed in reference [7] that the distribution during flexural vibration would be better approximated by constant body force loading, as might be applied by gravity, which leads to a linear variation (in the axial direction) of shearing force; this procedure led to shear coefficients in agreement with those in equations (1), and provided a formula involving the Saint-Venant flexure function suitable for other cross-sections. Of course, for MPT, there is no requirement for this second phase of the investigation, as all plates of uniform thickness have effectively the same cross-sectional shape, and the "best" shear coefficient should pertain to all plates.

In the case of plate flexural vibration, the exact benchmark with which MPT is here matched is the well known Rayleigh–Lamb theory [9, 10], and by using this truncation procedure, it is found that the "best" shear coefficient for the w_1 mode is

$$\kappa = 5/(6 - v). \tag{2}$$

With the benefit of hindsight, this value is not surprising, as it is exactly what one finds if Poisson ratio v in the *plane stress* thin rectangular beam coefficient of TBT, equation (1b), is replaced by $v/(1 - v)$, as would be required for a *plane strain* plate coefficient. Moreover, it is also the value arrived at by Hutchinson [11] who performed a similar analysis for a plate of circular planform, when the "exact" benchmark theory [12] was an infinite series solution in which the governing differential equations are satisfied identically, but the boundary conditions are approximated.

Comparisons are made between MPT phase velocity predictions for the lowest flexural (w_1) mode by using both this "best" coefficient and a range of coefficients employed by previous researchers, and with the exact Rayleigh–Lamb elastodynamic predictions; it is found that maximum error is approximately -0.5% when wavelength is equal to the plate thickness, which is a worthwhile improvement over the 3% error when using the popular value $\kappa = \pi^2/12$.

The second question is the validity of the higher spectra; for TBT, which predicts two frequency spectra (or two branches on a phase velocity/wavelength dispersion diagram), it was concluded in reference [13] that the second, higher, spectrum was "...an inevitable but meaningless consequence of the structure of an otherwise excellent approximate theory". The basis for that conclusion was a comparison between phase velocity predictions of TBT and the exact Pochhammer–Chree (PC) theory for an infinite beam of circular cross-section; for the first spectrum, the differences were not discernible on the dispersion diagram, and the maximum discrepancy was less than one-tenth of one percent over the wavelength range considered. However, for the second TBT spectrum, agreement could not be found over the same wavelength range; at long wavelength, one could enforce agreement with the second PC flexural mode with a suitable shear coefficient ($\kappa = 0.847$), but at short wavelength best agreement was afforded with the second PC longitudinal mode. Over the mid-range of wavelengths, one could not find any comparable exact prediction from PC theory.

The validity of the higher spectra of MPT, the w_2 and H modes (or thickness-shear and thickness-twist or breathing modes, respectively), has been called into question by

Levinson [14], as part of a study of a restricted exact elastodynamic plate solution based on a certain set of kinematic assumptions; whereas Levinson found good agreement between MPT and his exact theory for flexural frequencies—he concluded that "... the numerical predictions of MPT for the breathing frequencies are not particularly good approximations in general". More specifically, for the examples considered, there was reasonable agreement at the shorter wavelengths, but for the longer wavelengths there was an order of magnitude difference. Levinson dismissed the validity of the Mindlin H mode by referring to sketches of the mode in Mindlin's second paper on the subject, reference [2], in which plate thickness variation during oscillation contradicted the fundamental kinematic assumptions of MPT, and he expressed surprise that this had not been noted previously. (Of course, any inconsistency within Mindlin's papers is irrelevant: the acid test is whether there is agreement between the prediction and exact theory.) Levinson was less definite on the question of the w_2 mode of MPT; on the one hand he recognized that the mode had no analogue in his exact plate theory, but since the latter was based upon a restricted set of kinematic assumptions, it could not be assumed necessarily that there was no counterpart within the exact, and complete, three-dimensional theory. On the other hand, Levinson expected the w_2 mode to conform broadly with those kinematic assumptions, and therefore considered its existence to be rather dubious, indicating that an analysis of the type presented here would be necessary to settle the matter: indeed, it was precisely that observation which, belatedly, prompted the present work. By comparing MPT predictions with known exact theories, it will be seen that Levinson's doubts over the w_2 mode are quite justified, the mode displaying almost *schizophrenic* behaviour, by providing fair agreement with at least two different modes at various wavelengths. In contrast, it will be seen that the H mode is in exact agreement with frequency and phase (and therefore group) velocity predictions for the second slowest SH wave (see reference [15]) in the infinite plate as long as the shear coefficient takes the value $\kappa = \pi^2/12$. In arriving at his conclusion, Levinson appears to have overlooked these SH modes, which is not surprising since they have received comparatively little attention in the literature, as compared with the Rayleigh–Lamb modes. Both for completeness, and to partially remedy this imbalance, an outline derivation of the governing frequency equation is provided in Appendix 1.

Lastly in this Introduction, it is appropriate to note that there have been numerous studies on more "refined" shear deformation plate theories (see reference [16] for a brief review), the objectives of which have included the avoidance of shear coefficient usage, and the prediction of more realistic distributions of shear stress. An analysis of the structure of many of these alternative approximate theories has been provided recently by Muller and Touratier [17], but since these authors caution "Do not ask any of these two-dimensional plate theories to give you directly the exact thickness distribution of these shear-stresses", it would appear that avoidance of shear coefficient usage is the main advantage; however given the accuracy that MPT can achieve for the w_1 mode with the coefficient presented here, this advantage may be more imagined than real. Indeed, since in many of these theories, a shear coefficient is more or less implied in the choice of displacement field, it is likely that use of this "best" coefficient is effectively precluded.

2. MINDLIN PLATE THEORY EQUATIONS

For an unloaded simply supported rectangular plate occupying the space

$$0 \leqslant x \leqslant a, \qquad 0 \leqslant y \leqslant b, \qquad -h/2 \leqslant z \leqslant h/2, \tag{3}$$

undergoing natural oscillation at radian frequency ω, the Mindlin plate equations (see reference [18])

$$-\kappa Gh\left(\frac{\partial^2 w}{\partial x^2} + \frac{\partial^2 w}{\partial y^2} + \frac{\partial \beta_x}{\partial x} + \frac{\partial \beta_y}{\partial y}\right) + \rho h \frac{\partial^2 w}{\partial t^2} = 0,$$

$$\frac{D}{2}\left((1-v)\left(\frac{\partial^2 \beta_x}{\partial x^2} + \frac{\partial^2 \beta_x}{\partial y^2}\right) + (1+v)\frac{\partial}{\partial x}\left(\frac{\partial \beta_x}{\partial x} + \frac{\partial \beta_y}{\partial y}\right)\right) - \kappa Gh\left(\frac{\partial w}{\partial x} + \beta_x\right) - \frac{\rho h^3}{12}\frac{\partial^2 \beta_x}{\partial t^2} = 0,$$

$$\frac{D}{2}\left((1-v)\left(\frac{\partial^2 \beta_y}{\partial x^2} + \frac{\partial^2 \beta_y}{\partial y^2}\right) + (1+v)\frac{\partial}{\partial y}\left(\frac{\partial \beta_x}{\partial x} + \frac{\partial \beta_y}{\partial y}\right)\right) - \kappa Gh\left(\frac{\partial w}{\partial y} + \beta_y\right) - \frac{\rho h^3}{12}\frac{\partial^2 \beta_y}{\partial t^2} = 0,$$

$$(4)$$

reduce to the form

$$\begin{bmatrix} a_{11} - \rho h\omega^2 & a_{12} & a_{13} \\ a_{21} & a_{22} - \dfrac{\rho h^3}{12}\omega^2 & a_{23} \\ a_{31} & a_{32} & a_{33} - \dfrac{\rho h^3}{12}\omega^2 \end{bmatrix}\begin{bmatrix} A_{mn} \\ B_{mn} \\ C_{mn} \end{bmatrix} = 0, \qquad (5)$$

where

$$a_{11} = \kappa Gh\left[\left(\frac{m\pi}{a}\right)^2 + \left(\frac{n\pi}{b}\right)^2\right], \qquad a_{22} = D\left[\left(\frac{m\pi}{a}\right)^2 + \frac{(1-v)}{2}\left(\frac{n\pi}{b}\right)^2\right] + \kappa Gh,$$

$$a_{33} = D\left[\frac{(1-v)}{2}\left(\frac{m\pi}{a}\right)^2 + \left(\frac{n\pi}{b}\right)^2\right] + \kappa Gh, \qquad a_{12} = a_{21} = \kappa Gh\left(\frac{m\pi}{a}\right),$$

$$a_{13} = a_{31} = \kappa Gh\left(\frac{n\pi}{b}\right), \qquad a_{23} = a_{32} = D\frac{(1+v)}{2}\left(\frac{m\pi}{a}\right)\left(\frac{n\pi}{b}\right). \qquad (6)$$

In these equations κ, G, ρ and v are the shear coefficient, the shear modulus, the mass density and the Poisson's ratio, respectively; D is the plate flexural rigidity, given by

$$D = Eh^3/12(1 - v^2) = Gh^3/6(1 - v), \qquad (7)$$

and E is Young's modulus; it has been assumed that the plate centre line deflection w and the rotations β_x and β_y are given by

$$w = A_{mn}\sin\frac{m\pi x}{a}\sin\frac{n\pi y}{b}, \qquad \beta_x = B_{mn}\cos\frac{m\pi x}{a}\sin\frac{n\pi y}{b}, \qquad \beta_y = C_{mn}\sin\frac{m\pi x}{a}\cos\frac{n\pi y}{b}, \qquad (8)$$

where A_{mn}, B_{mn}, and C_{mn} are constants pertaining to the mnth case, and the time dependency $\exp(i\omega t)$ is assumed. It should be noted that the x–y dependency assumed in equations (8) satisfies the required boundary conditions at the simply supported edges of the plate, and is also compatible with a standing or travelling wave in a plate of infinite extent.

Setting the determinant in equation (5) to zero leads to a cubic equation in ω^2, which factorizes to give the quadratic in ω^2 as

$$\rho h^3 \omega^4 - \omega^2(12\pi^2 DM^2 + 12\kappa Gh + \pi^2 M^2 \kappa Gh^3) + 12\pi^4 M^4 D\kappa G/\rho = 0, \qquad (9)$$

together with

$$\omega^2 = \{12\kappa Gh + 6\pi^2 M^2 D(1-v)\}/\rho h^3, \qquad (10)$$

where the notation

$$M^2 = (m/a)^2 + (n/b)^2 \qquad (11)$$

has been employed.

Application of the quadratic formula to equation (9) leads to frequency predictions for the w_1 and w_2 modes, while equation (10) gives the frequency of the H mode.

2.1. FIRST AND SECOND ORDER PHASE VELOCITY APPROXIMATIONS TO THE w_1 MODE

Upon setting $\omega = \varkappa c_p$, where $\varkappa = 2\pi/\lambda = \pi/\Gamma$ is the wavenumber, λ is wavelength, c_p is the phase velocity, and Γ is the semi-wavelength, equation (9) may be written in the non-dimensional form

$$\left(\frac{c_p}{c_s}\right)^4 \left(\frac{h}{\Gamma}\right)^4 - \left(\frac{c_p}{c_s}\right)^2 \left(\frac{h}{\Gamma}\right)^2 \left[\frac{12\kappa}{\pi^2} + \left(\frac{h}{\Gamma}\right)^2 \left(\kappa + \frac{2}{1-v}\right)\right] + \frac{2\kappa}{1-v}\left(\frac{h}{\Gamma}\right)^4 = 0. \qquad (12)$$

Note here that M as defined by equation (11) is in fact the inverse of the semi-wavelength Γ, and $c_s = (G/\rho)^{1/2}$ is the shear wave velocity.

One can now note that the terms c_p/c_s and h/Γ are, for the long wavelength approximation, both small quantities, both of whose order of magnitude is denoted by Δ. The first order approximation is obtained by omitting terms of order higher than Δ^4, which effectively means ignoring the first and part of the second term in equation (12) to give just

$$\left(\frac{c_p}{c_s}\right) = \frac{\pi}{\sqrt{6(1-v)}}\left(\frac{h}{\Gamma}\right), \qquad (13)$$

and this agrees with the phase velocity prediction of classical thin plate theory (TPT). It is immediately apparent that TPT gives the physically unrealistic prediction that $c_p/c_s \rightarrow \infty$ as $h/\Gamma \rightarrow \infty$, and it was this observation (or rather a parallel observation for Euler–Bernoulli beam theory) which provided the original motivation for the introduction of first rotatory inertia and then shear deformation effects, such that the limiting velocity at short wavelength would be that of, or at least close to, Rayleigh surface waves.

For the second order approximation, terms of order higher than Δ^6 are omitted, which is just the first term in equation (12), which gives

$$\left(\frac{c_p}{c_s}\right) = \frac{\pi}{\sqrt{6(1-v)}}\left(\frac{h}{\Gamma}\right)\left[1 + \frac{\pi^2}{12}\left(\frac{h}{\Gamma}\right)^2\left(1 + \frac{2}{\kappa(1-v)}\right)\right]^{-1/2}; \qquad (14)$$

employing the binomial expansion, and omitting terms of order higher than Δ^3 gives the second order approximation as

$$\left(\frac{c_p}{c_s}\right) = \frac{\pi}{\sqrt{6(1-v)}} \left(\frac{h}{\Gamma}\right)\left[1 - \frac{\pi^2}{12}\left(\frac{h}{\Gamma}\right)^2\left(\frac{1}{2} + \frac{1}{\kappa(1-v)}\right)\right]. \tag{15}$$

2.2. RAYLEIGH–LAMB FREQUENCY EQUATION: FIRST AND SECOND ORDER APPROXIMATIONS

The exact Rayleigh–Lamb frequency equation for the infinite plate can be written in the form

$$\frac{\tan\left(\frac{\pi}{2}\left(\frac{h}{\Gamma}\right)\left(\left(\frac{c_p}{c_s}\right)^2 - 1\right)^{1/2}\right)}{\tan\left(\frac{\pi}{2}\left(\frac{h}{\Gamma}\right)\left(\left(\frac{c_p}{kc_s}\right)^2 - 1\right)^{1/2}\right)} + \left[\frac{4\left(\left(\frac{c_p}{c_s}\right)^2 - 1\right)^{1/2}\left(\left(\frac{c_p}{kc_s}\right)^2 - 1\right)^{1/2}}{\left(2 - \left(\frac{c_p}{c_s}\right)^2\right)^2}\right]^{\pm 1} = 0, \tag{16}$$

where

$$k^2 = 2(1-v)/(1-2v), \tag{17}$$

and the exponents ± 1 pertain to symmetric and asymmetric modes respectively; for the lowest, flexural, mode one requires the latter.

Employing three terms in the ascending series for the tangent functions, cancelling the factor h/Γ, and omitting terms of order higher than Δ^4 leads to the first order approximation

$$\left(\frac{c_p}{c_s}\right) = \frac{\pi}{\sqrt{6(1-v)}}\left(\frac{h}{\Gamma}\right), \tag{18}$$

which is in agreement with classical thin plate theory. The second order approximation is obtained by omitting terms of order greater than Δ^6, which leads to the prediction

$$\left(\frac{c_p}{c_s}\right) = \frac{\pi}{\sqrt{6(1-v)}}\left(\frac{h}{\Gamma}\right)\left[1 - \frac{\pi^2}{5}\left(\frac{h}{\Gamma}\right)^2\right]^{1/2}\left[1 + \frac{\pi^2}{12}\left(\frac{h}{\Gamma}\right)^2\left(\frac{1+v}{1-v}\right)\right]^{-1/2}. \tag{19}$$

Employing the binomial expansion, and now omitting terms higher than Δ^3 gives the second order approximation as

$$\left(\frac{c_p}{c_s}\right) = \frac{\pi}{\sqrt{6(1-v)}}\left(\frac{h}{\Gamma}\right)\left[1 - \frac{\pi^2}{12}\left(\frac{h}{\Gamma}\right)^2\left(\frac{1+v}{2(1-v)} + \frac{6}{5}\right)\right]. \tag{20}$$

One now requires that these two second order approximations, equations (15) and (20), should be identical which yields the value for the shear coefficient κ as

$$\kappa = 5/(6-v). \tag{21}$$

For completeness, this and previous plate shear coefficients, together with their originators, are listed below, or shown in Table 1 for those values having a Poisson ratio dependence.

TABLE 1

Shear coefficients dependent on the Poisson ratio; c_R denotes the Rayleigh surface wave velocity

Poisson ratio, v	0·0	0·25	0·3	0·5
$\kappa = (c_R/c_s)^2$ (Mindlin [1])	0·763932	0·845299	0·860094	0·912622
$\kappa = 5/(6 - v)$ (Hutchinson [11], present author)	0·833333	0·869565	0·877193	0·909091

Numerically, the differences may not be large but, as will be seen, the effect on phase velocity prediction can be significant. The listed values are as follows:

$$\kappa = 2/3 = 0\cdot666667, \text{ Uflyand [19]}; \quad \kappa = 5/6 = 0\cdot833333, \text{ Reissner [20]};$$

$$\kappa = \pi^2/12 = 0\cdot822467, \text{ Mindlin [2]}; \quad \kappa = 8/9 = 0\cdot888889, \text{ Timoshenko*}.$$

3. THEORETICAL PREDICTIONS

3.1. PHASE VELOCITIES DISPERSION DIAGRAM

Exact phase velocity predictions from the Rayleigh–Lamb (R–L) frequency equation are shown as solid lines in Figure 1, while predictions from Mindlin plate theory (MPT), thin plate theory (TPT) and various asymptotic or reference velocities are shown using a variety of characters. First, it is noted that TPT provides perfectly acceptable agreement with the exact flexural mode for long (non-dimensional) wavelength, that is for $h/\Gamma < 0\cdot2$; for shorter wavelengths, the w_1 mode of MPT (with $\kappa = 5/(6 - v)$), marked with an asterisk, provides such excellent agreement that no error can be discerned on the diagram. Actual errors between the two predictions, for various values of the Poisson ratio, will be considered later in more depth; however, at this point in the discussion it suffices to note that there is excellent agreement throughout the range considered; note that $h/\Gamma = 2$ is equivalent to a wavelength equal to plate thickness, and the elastic body might more properly be considered a block rather than a plate. As the wavelength approaches zero for this mode, so the exact elastodynamic theory predicts that disturbances should propagate at the Rayleigh surface wave velocity (RSWV), $c_p/c_s = 0\cdot9274$, for a Poisson's ratio of $v = 0\cdot3$. For the particular shear coefficient employed in Figure 1, $\kappa = 5/(6 - v)$, the difference in prediction between exact and MPT is $0\cdot989\%$, as the semi-wavelength Γ approaches zero; this error could be brought to zero by choosing a shear coefficient such that agreement between MPT and RSWV, as Γ approaches zero, is enforced. This is the approach first adopted by Mindlin [1], and requires use of the coefficient $\kappa = 0\cdot860094$ for $v = 0\cdot3$, as in Table 1; however, as will be seen, this value of the shear coefficient provides less good agreement over the longer wavelength range, although it is better than the coefficient $\kappa = \pi^2/12$, which Mindlin employed in his second paper [2]. Moreover, if one is interested only in the limiting case of the velocity as the wavelength approaches zero, there is little point in *not* using the well known RSWV prediction but rather relying on MPT to predict this limiting behaviour, especially as one could hardly expect the assumed displacement field of MPT to approximate that of a Rayleigh surface wave; the present author is therefore of the opinion that this approach to choosing the best shear coefficient serves little or no purpose.

---

* This value has a long but rather obscure history, considered in some detail in Appendix 2.

The slowest symmetric branch (that is, employing the exponent $+1$ in equation (16)) is that of the thickness-shear mode, denoted by TS in Figure 1, and has $c_p/c_s = 1$ for all wavelengths. The second slowest symmetric (longitudinal) prediction from R–L theory, denoted by an L on Figure 1, has non-dimensional phase velocity $c_p/c_s = 1\cdot6903$ at zero wavelength, which is equivalent to the bar velocity, $(E/\rho)^{1/2}$, but with the value of Young's modulus E replaced by $E/(1 - v^2)$, as is consistent with a plane strain condition. As with the lowest asymmetric mode (the flexural mode), the short wavelength limiting velocity is RSWV. Also shown, for reference purposes, are the velocity of waves of dilatation for the infinite region, which has $c_p/c_s = (2(1 - v)/(1 - 2v))^{1/2} = (3\cdot5)^{1/2} \approx 1\cdot8708$, for a Poisson's ratio of $v = 0\cdot3$, and that of RSWV which has $c_p/c_s = 0.9274$; both of these are shown as dotted lines in Figure 1. Higher exact branches from R–L theory occur in "pairs", and are denoted by an S or an A according to whether they are symmetric or asymmetric.

Now consider the w_2 mode of MPT, marked by a cross in Figure 1. At long wavelength, $h/\Gamma \leqslant 0\cdot5$, there is reasonable agreement with an asymmetric mode of R–L, while at shorter wavelength, $h/\Gamma \geqslant 0\cdot9$, there is better agreement with a higher R–L symmetric mode. In the limit $h/\Gamma \rightarrow \infty$, the w_2 mode has $c_p/c_s = 1\cdot6903$, whereas the above and higher R–L mode velocities approach the velocity of waves of distortion, c_s. Thus it would appear that the w_2 prediction cannot be associated with a single mode from exact elastodynamic theory throughout the wavelength range; indeed in the wavelength range in Figure 1 it is close to, or crosses four exact R–L or SH modes at various wavelengths, and as $h/\Gamma \rightarrow \infty$, so the mode will provide exact agreement with an infinite number of exact modes *at discrete values of h/Γ*; that is, where the w_2 mode crosses the exact R–L modes, as the latter approach c_s. In view of this *schizophrenic* nature of the phase velocity predictions of this mode, they should be disregarded.

At first sight, the H mode (calculated with the shear coefficient $\kappa = \pi^2/12$), denoted by H in Figure 1, is likewise close to the second slowest asymmetric R–L mode at long wavelength, before showing good agreement with the lowest symmetric (longitudinal)
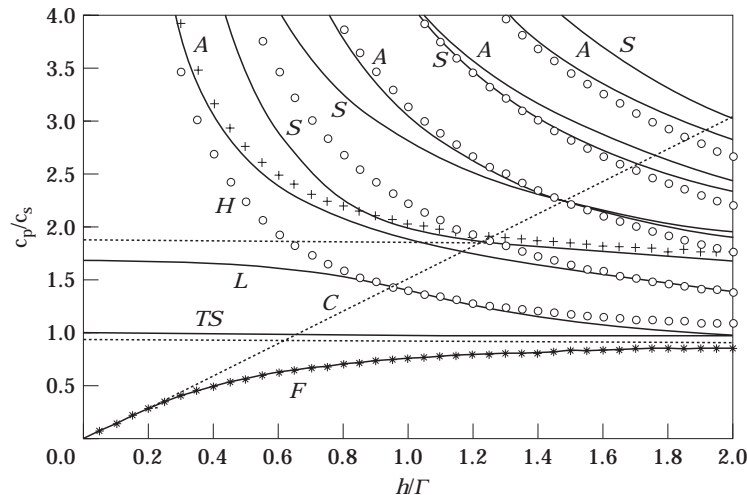

Figure 1. A dispersion diagram for Rayleigh–Lamb, Mindlin, SH and classical thin plate theories: non-dimensional phase velocity (c_p/c_s) versus plate thickness/semi-wavelength (h/Γ). The Poisson's ratio $v = 0\cdot3$. Exact R–L predictions are shown as solid lines; *, w_1 mode; $\circ$, SH modes; $+$, w_2 mode. RSWV, and the velocity of waves of dilatation in the infinite medium, are shown as dotted lines, as is the prediction of classical plate theory, also marked with the letter C. F, TS, L, H, A and S label flexural, thickness shear, longitudinal, H mode, asymmetric and symmetric modes, respectively.
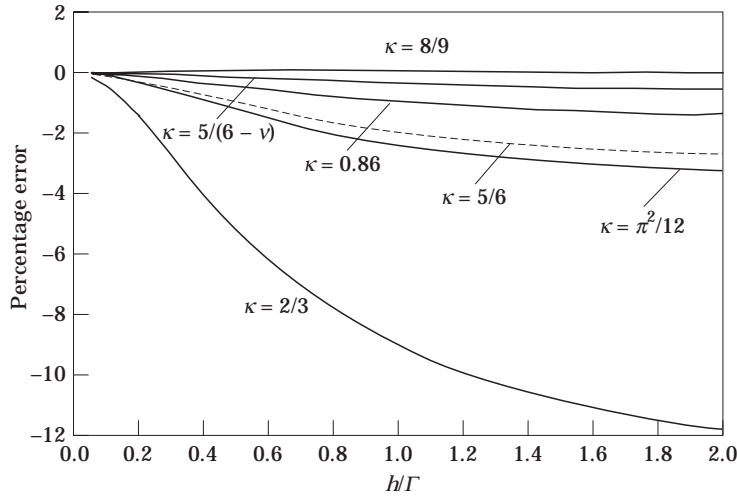
Figure 2. The percentage error in the w_1 mode for various shear coefficients; Poisson ratio $v = 0.3$.

mode for $0.8 \geqslant h/\Gamma \geqslant 1.2$, and it is tempting also to dismiss the Mindlin prediction on the basis of its schizophrenic behaviour. In fact, this mode is just one of a family of exact *SH* modes, all of which are marked by a circle in Figure 1; the common feature of this *SH* mode is that the transverse displacement, w, is zero, and its derivation and equivalence to the Mindlin H mode is demonstrated in Appendix 1. All of these modes have velocities approaching c_s as wavelength approaches zero.

3.2. ERRORS IN FLEXURAL, w_1, MODE FOR VARIOUS SHEAR COEFFICIENTS

As has been remarked above, there is no discernible difference between the w_1 mode of MPT and the flexural branch of R–L theory on the dispersion diagram, Figure 1; in this section, percentage errors between the two are considered for a variety of shear coefficients, for two values of the Poisson ratio. In Figure 2 is shown the percentage error for a Poisson's ratio $v = 0.3$; it is immediately evident that the value $\kappa = 5/(6 - v)$ provides best
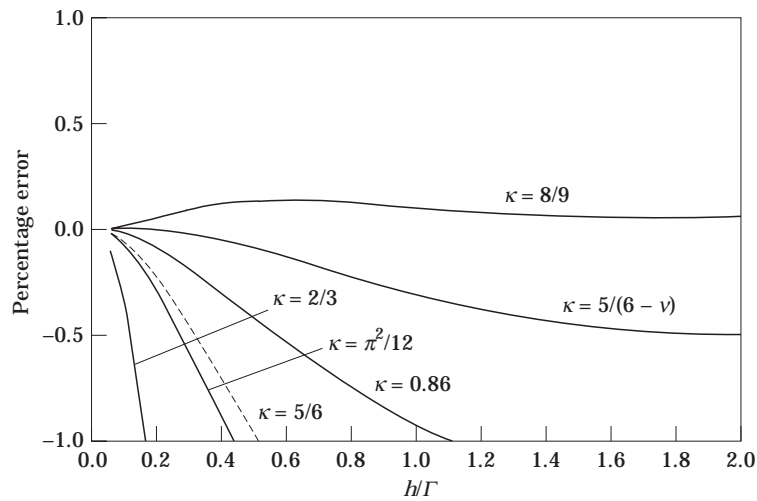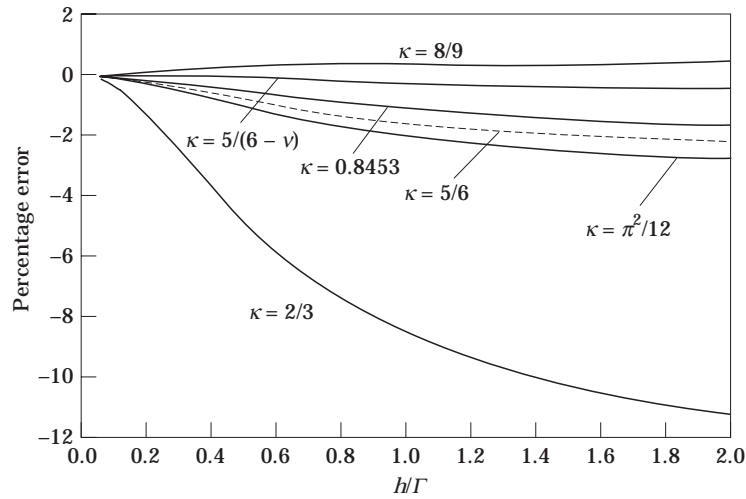

Figure 3. A "close up" of Figure 2.

Figure 4. The percentage error in the w_1 mode for various shear coefficients; Poisson ratio $v = 0.25$.

agreement over the wavelength range considered, with the one surprising exception of the value $\kappa = 8/9$. For $h/\Gamma = 2$, when the wavelength is equal to the plate depth, the popular value of $\kappa = \pi^2/12$ gives an error in excess of -3%, while the value $\kappa = 2/3$ gives an error approaching -12%. The value $\kappa = 5/(6 - v)$ gives an error of approximately -0.5% and, as has been seen above, there is an error of less than $+1\%$ as $h/\Gamma \to \infty$. The surprising result is the case of $\kappa = 8/9$, where the maximum error over the wavelength range of Figure 2 is approximately 0.14%, and the error is just 0.064% as $h/\Gamma = 2$, as can be seen in Figure 3 which is a "close-up" of Figure 2; as $h/\Gamma \to \infty$, the error is $+1.66\%$, which is slightly worse than the prediction with $\kappa = 5/(6 - v)$. This value, however, suffers from being independent of the Poisson's ratio, and this better agreement should be regarded as fortuitous. Thus in Figures 4 and 5, which show errors for Poisson's ratio $v = 0.25$, the general error trends are similar, but best agreement is now given by the value $\kappa = 5/(6 - v)$, with maximum error smaller than -0.5%, while the value $\kappa = 8/9$ gives an error in excess
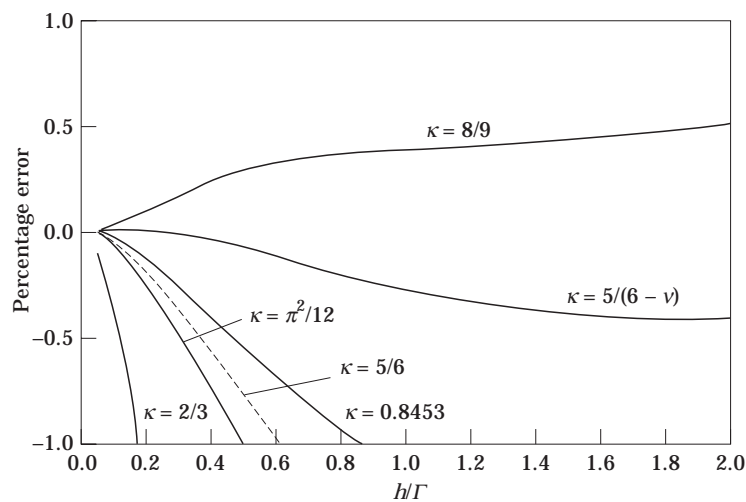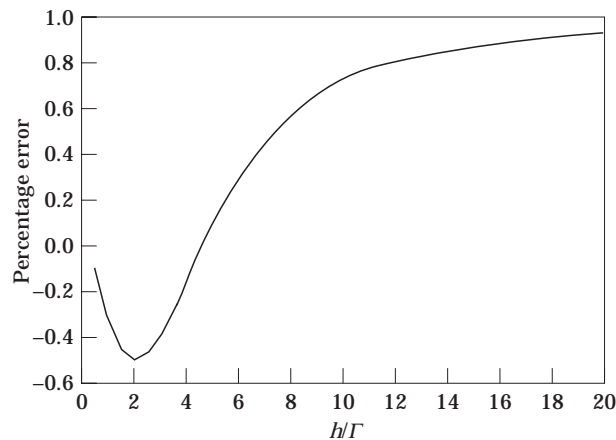

Figure 5. A "close up" of Figure 4.

Figure 6. The percentage error in the w_1 mode for $\kappa = 5/(6 - v)$ over the wavelength range $0 \leqslant h/\Gamma \leqslant 20$; Poisson's ratio $v = 0.3$.

of $+0.5\%$, for $h/\Gamma = 2$. For completeness, the w_1 mode error employing the coefficient $\kappa = 5/(6 - v)$, with $v = 0.3$, is shown in Figure 6 over the wavelength range $0 \leqslant h/\Gamma \leqslant 20$, and indicates the transition from slight underestimate at long wavelength to slight overestimate at short wavelength; these results are in complete qualitative agreement with those of Hutchinson [11], who found that a coefficient slightly in excess of $\kappa = 5/(6 - v)$ at long wavelength, and slightly smaller at short wavelength, would provide exact agreement between MPT and his "exact" elasticity solution [12].

4. CONCLUSIONS

By matching long wavelength phase velocity predictions between the w_1 mode of Mindlin plate theory and the exact Rayleigh–Lamb frequency equation for flexural waves, a best shear coefficient of $\kappa = 5/(6 - v)$ is found; when employing this value, the Mindlin w_1 mode has less than -0.5% error in phase velocity prediction, when the wavelength approaches the plate thickness, and maximum 1% error as wavelength approaches zero. The Mindlin H mode, previously dismissed by Levinson, provides exact agreement with the second slowest of a family of SH waves for the infinite plate, as long as the shear coefficient takes the value $\kappa = \pi^2/12$. The Mindlin w_2 mode, however, cannot be reconciled with any known single exact elastodynamic mode, and should therefore be disregarded.

REFERENCES

1. R. D. MINDLIN 1951 *Transactions of the American Society of Mechanical Engineers*, *Journal of Applied Mechanics* **18**, 31–38. Influence of rotatory inertia and shear on flexural motions of isotropic elastic plates.
2. R. D. MINDLIN, A. SCHACKNOW and H. DERESIEWICZ 1956 *Transactions of the American Society of Mechanical Engineers*, *Journal of Applied Mechanics* **23**, 430–436. Flexural vibrations of rectangular plates.
3. N. G. STEPHEN 1981 *International Journal of Solids and Structures* **17**, 325–333. Considerations on second order beam theories.
4. E. E. ZAJAC 1962 in *Handbook of Engineering Mechanics* (W. Flügge, editor). New York: McGraw-Hill. See chapter 64: Propagation of elastic waves.
5. G. R. COWPER 1968 *American Society of Civil Engineers*, *Journal of the Engineering Mechanics Division* **94**, EM6, 1447–1453. On the accuracy of Timoshenko's beam theory.

6. T. KANEKO 1975 *Journal of Physics D*: *Applied Physics* **8**, 1927–1939. On Timoshenko's correction for shear in vibrating beams.

7. N. G. STEPHEN and M. LEVINSON 1979 *Journal of Sound and Vibration* **67**, 293–305. A second order beam theory.

8. G. R. COWPER 1966 *Transactions of the American Society of Mechanical Engineers*, *Journal of Applied Mechanics* **33**, 335–340. The shear coefficient in Timoshenko's beam theory.

9. LORD RAYLEIGH 1889 *Proceedings of the London Mathematical Society* **10**, 225–234. On the free vibrations of an infinite plate of homogenous elastic material.

10. H. LAMB 1917 *Proceedings of the Royal Society* **A93**, 114–128. On waves in an elastic plate.

11. J. R. HUTCHINSON 1984 *Transactions of the American Society of Mechanical Engineers*, *Journal of Applied Mechanics* **51**, 581–585. Vibrations of thick free circular plates, exact versus approximate solutions.

12. J. R. HUTCHINSON 1980 *Transactions of the American Society of Mechanical Engineers*, *Journal of Applied Mechanics* **47**, 901–907. Vibrations of solid cylinders.

13. N. G. STEPHEN 1982 *Journal of Sound and Vibration* **80**, 578–582. The second frequency spectrum of Timoshenko beams.

14. M. LEVINSON 1985 *Journal of Sound and Vibration* **98**, 289–298. Free vibrations of a simply supported, rectangular plate: an exact elasticity solution.

15. J. MIKLOWITZ 1978 *The Theory of Elastic Waves and Waveguides*. Amsterdam: North-Holland. See article 4.2, pages 209–211.

16. G. JEMIELITA 1990 *Transactions of the American Society of Mechanical Engineers*, *Journal of Applied Mechanics* **57**, 1088–1091. On kinematical assumptions of refined theories of plates: a survey.

17. P. MULLER and M. TOURATIER 1996 *Journal of Sound and Vibration* **188**, 515–527. On the so-called variational consistency of plate models, I. Indefinite plates: evaluation of dispersive behaviour.

18. W. SOEDEL 1993 *Vibrations of Shells and Plates*. New York: Dekker; second edition. See pages 279–283.

19. Y. S. UFLYAND 1948 *Prikladnaia Mathematika i Mekhanica* **12**, 287–300. The propagation of waves in the transverse vibrations of bars and plates. (In Russian.)

20. E. REISSNER 1947 *Quarterly of Applied Mathematics* **5**, 55–68. On bending of elastic plates.

21. S. SRINIVAS, C. V. JOGA RAO and A. K. RAO 1970 *Journal of Sound and Vibration* **12**, 187–199. An exact analysis for vibration of simply-supported homogeneous and laminated thick rectangular plates.

22. S. P. TIMOSHENKO 1992 *Philosophical Magazine* (series 6) **43**, 125–131. On the transverse vibrations of bars of uniform cross-section.

23. A. E. H. LOVE 1944 *A Treatise on the Mathematical Theory of Elasticity*. New York: Dover, fourth edition. See articles 245 and 245A.

24. L. N. G. FILON 1903 *Philosophical Transactions of the Royal Society* **A201**, 63–155. On an approximate solution for the bending of a beam of rectangular cross-section under any system of load, with special reference to points of concentrated or discontinuous loading.

25. L. N. G. FILON 1903 *Philosophical Magazine* (series 6) **23**, 1–25. The investigation of stresses in a rectangular bar by means of polarised light.

26. S. P. TIMOSHENKO 1955 *Strength of Materials*, Volume 1. New York: Van Nostrand, third edition. See page 174.

APPENDIX 1: *SH* WAVES IN THE INFINITE PLATE

The starting point is the displacement equations of motion

$$\frac{G}{1-2v}\frac{\partial e}{\partial x} + G\mathbf{V}^2 u = \rho\frac{\partial^2 u}{\partial t^2}, \quad \frac{G}{1-2v}\frac{\partial e}{\partial y} + G\mathbf{V}^2 v = \rho\frac{\partial^2 v}{\partial t^2}, \quad \frac{G}{1-2v}\frac{\partial e}{\partial z} + G\mathbf{V}^2 w = \rho\frac{\partial^2 w}{\partial t^2},$$

$$(A1a\text{–}c)$$

where e is the dilatation, given by

$$e = \partial u/\partial x + \partial v/\partial y + \partial w/\partial z; \tag{A2}$$

the assumption $w = 0$ in equation (A1c) leads to the condition

$$(\partial/\partial z)(\partial u/\partial x + \partial v/\partial y) = 0. \tag{A3}$$

Since the stress σ_z is zero on the boundary, it will be seen that this condition implies that this stress is zero throughout the plate.

Writing

$$u(x, y, z, t) = U(z) \exp\left(\frac{im\pi x}{a} + \frac{in\pi y}{b} + i\omega t\right),$$

$$v(x, y, z, t) = V(z) \exp\left(\frac{im\pi x}{a} + \frac{in\pi y}{b} + i\omega t\right), \tag{A4}$$

in equations (A1a,b) leads to the two coupled ordinary differential equations

$$\frac{d^2 U(z)}{dz^2} + \left(\frac{\rho\omega^2}{G} - \left(\frac{m\pi}{a}\right)^2 - \left(\frac{n\pi}{b}\right)^2 - \frac{1}{1 - 2v}\left(\frac{m\pi}{a}\right)^2\right)U(z) - \frac{1}{1 - 2v}\left(\frac{m\pi}{a}\right)\left(\frac{n\pi}{b}\right)V(z) = 0, \tag{A5a}$$

$$\frac{d^2 V(z)}{dz^2} + \left(\frac{\rho\omega^2}{G} - \left(\frac{m\pi}{a}\right)^2 - \left(\frac{n\pi}{b}\right)^2 - \frac{1}{1 - 2v}\left(\frac{n\pi}{b}\right)^2\right)V(z) - \frac{1}{1 - 2v}\left(\frac{m\pi}{a}\right)\left(\frac{n\pi}{b}\right)U(z) = 0. \tag{A5b}$$

Setting

$$U(z) = \bar{U} \exp(\lambda z), \qquad V(z) = \bar{V} \exp(\lambda z) \tag{A6}$$

leads to a characteristic equation which factorizes as

$$(\lambda_1^2 - (\pi/\Gamma)^2 + (\omega/c_s)^2)(\lambda_2^2 - (\pi k/\Gamma)^2 + (\omega/c_s)^2) = 0. \tag{A7}$$

Under the assumption that λ_1 and λ_2 are both positive, one has

$$U(z) = U_1 \cosh \lambda_1 z + U_2 \sinh \lambda_1 z + U_3 \cosh \lambda_2 z + U_4 \sinh \lambda_2 z,$$

$$V(z) = V_1 \cosh \lambda_1 z + V_2 \sinh \lambda_1 z + V_3 \cosh \lambda_2 z + V_4 \sinh \lambda_2 z. \tag{A8}$$

However, the eight constants in equations (A8) cannot be independent, and back substitution into either of equations (A5) leads to the relationships

$$\frac{m}{a} U_1 + \frac{n}{b} V_1 = 0, \qquad \frac{m}{a} U_2 + \frac{n}{b} V_2 = 0, \qquad \frac{m}{a} V_3 - \frac{n}{b} U_3 = 0, \qquad \frac{m}{a} V_4 - \frac{n}{b} U_4 = 0. \tag{A9}$$

One now considers the side-condition for $w = 0$, equation (A3). Substituting from (A8) leads to the requirement, valid throughout the thickness,

$$\lambda_2(b/n)M^2(V_3 \sinh \lambda_2 z + V_4 \cosh \lambda_2 z) = 0. \tag{A10}$$

This condition requires either $\lambda_2 = 0$—in which case $U(z)$ and $V(z)$ are independent of constants U_4 and V_4, and U_3 and V_3 are rigid body displacements, and therefore irrelevant—or $V_3 = V_4 = 0$, which in turn requires $U_3 = U_4 = 0$. In either case, these constants are zero, and the functions $U(z)$ and $V(z)$ become

$$U(z) = U_1 \cosh \lambda_1 z + U_2 \sinh \lambda_1 z, \qquad V(z) = -(bm/na)U(z). \tag{A11}$$

The traction-free boundary conditions on the upper and lower surfaces of the plate, that is

$$\sigma_z = \tau_{xz} = \tau_{yz} = 0 \qquad \text{on } z = \pm h/2, \tag{A12}$$

become, respectively,

$$(m/a)U(z) + (n/b)V(z) = 0, \qquad dU(z)/dz = 0, \qquad dV(z)/dz = 0. \tag{A13a–c}$$

The boundary condition (A13a) is satisfied identically, while the two others both reduce to

$$\begin{bmatrix} \sinh(\lambda_1 h/2) & \cosh(\lambda_1 h/2) \\ -\sinh(\lambda_1 h/2) & \cosh(\lambda_1 h/2) \end{bmatrix} \begin{bmatrix} U_1 \\ U_2 \end{bmatrix} = 0, \tag{A14}$$

and setting the determinant equal to zero gives the frequency equation

$$\sinh \lambda_1 h = 0. \tag{A15}$$

If λ_1 is real, then the only root is $\lambda_1 h = 0$, which is a special case of λ_1 being imaginary, whereupon the frequency equation may be written as

$$\sin \sqrt{\left(\frac{\omega h}{c_s}\right)^2 - \left(\frac{\pi h}{\Gamma}\right)^2} = 0, \qquad \left(\frac{\omega h}{c_s}\right)^2 - \left(\frac{\pi h}{\Gamma}\right)^2 = n^2\pi^2, \qquad n = 0,1,2,\ldots, \tag{A16}$$

or

$$\omega^2 = (Gn^2\pi^2 h + G\pi^2 M^2 h^3)/\rho h^3, \tag{A17}$$

where M has replaced Γ^{-1}.

For $n = 0$, the frequency is that of simple thickness-shear, with phase velocity equal to c_s; for $n = 1$, the frequency is identical to the Mindlin H mode prediction, equation (10), provided that the shear coefficient in the latter takes the value $\kappa = \pi^2/12$. The phase velocity for this mode reduces to the simple form

$$(c_p/c_s)^2 = 1 + n^2(h/\Gamma)^{-2}, \tag{A18}$$

Finally in this Appendix, it should be noted that Srinivas et al. [21] briefly mentioned this mode as part of a larger study of vibration in thick plates of rectangular planform, performing an analysis similar in nature to that of Hutchinson [12], and likewise concluded that the H mode frequency prediction was exact as long as one employes the coefficient $\kappa = \pi^2/12$. On the other hand, those authors concluded that the Mindlin w_2 mode eigenvalues were only slightly greater than those of an exact asymmetric mode, and was therefore valid for frequency (or phase velocity) prediction; the present work suggests otherwise.

APPENDIX 2

Mindlin [1] attributed both the values $\kappa = 2/3$ and $8/9$ to Timoshenko, the latter value having rather an interesting history. It was employed by Timoshenko in 1922 [22] in a paper which compares the long wavelength prediction of Timoshenko beam theory (TBT) with exact elasticity solutions for both the bar of circular cross-section, and the Rayleigh–Lamb plate equation for a "wide", that is plane strain, beam of rectangular cross-section. Timoshenko in turn attributed this value to an experimental (photoelastic) study by Filon, referring the reader to an article on the effect of surface loading of beams

in Love's treatise [23], and in particular the departure from the Euler–Bernoulli relationship of proportionality between bending moment and curvature through the so-called "additional deflection due to shear". Love refers the reader to a theoretical study by Filon [24], which has in turn been verified experimentally by Filon [25].

According to Filon's theoretical study, the central deflection δ of a simply supported beam of length L, depth d, and having flexural rigidity EI, loaded by a concentrated load W at midspan, can be written as

$$\delta = \frac{WL^3}{48EI}\left(1 + \frac{3}{20}(16 + 10v)\frac{d^2}{L^2}\right). \tag{B1}$$

The first term is the usual "strength of materials" deflection, while the second gives the additional deflection due to shear. Timoshenko quotes the correcting factor in his text [26] as

$$\left(1 + 2\cdot85\frac{d^2}{L^2}\right), \tag{B2}$$

implying a choice of Poisson's ratio as $v = 0\cdot3$, while Love has the same correcting factor as

$$\left(1 + \frac{45}{16}\frac{d^2}{L^2}\right), \tag{B3}$$

which implies $v = 11/40$, this being an acceptable value for the glass employed in Filon's experimental study. A shear coefficient of $\kappa = 8/9$ can be arrived at by equating the "strength of materials" estimate of the correcting factor, which is

$$\left(1 + \frac{E}{\kappa G}\frac{d^2}{L^2}\right), \tag{B4}$$

with the factor quoted by Love, expression (B3), and setting the Poisson's ratio $v = 0\cdot25$ (rather than $11/40$): this would appear to be the procedure adopted by Timoshenko in reference [22]. If this inconsistency of two different values of the Poisson's ratio is removed, by equating factors (B1) and (B4), then the resulting coefficient is

$$\kappa = \frac{20(1 + v)}{24 + 15v}, \tag{B5}$$

which is equal to $8/9$ for $v = 0\cdot2$.

However, it should be noted that the above calculations pertain to a thin, that is plane stress, rectangular cross-section: the "true" plate coefficient from this approach is obtained by replacing the Poisson's ratio v in equation (B5) by $v/(1 - v)$, to give

$$\kappa = \frac{20}{24 - 9v}. \tag{B6}$$

Phase velocity predictions for the w_1 mode when using this value of the coefficient are not shown in Figures 2–5; however, the error characteristic is similar to that when using the value $\kappa = 5/6$, except that it is positive rather than negative.